

## Article

# Innovative Polymer Microspheres with Chloride Groups Synthesis, Characterization and Application for Dye Removal

Monika Wawrzkievicz <sup>1,\*</sup>  and Beata Podkościelna <sup>2</sup> 

<sup>1</sup> Department of Inorganic Chemistry, Institute of Chemical Sciences, Faculty of Chemistry, Maria Curie-Skłodowska University in Lublin, M. Curie-Skłodowska Sq. 2, 20-031 Lublin, Poland

<sup>2</sup> Department of Polymer Chemistry, Institute of Chemical Sciences, Faculty of Chemistry, Maria Curie-Skłodowska University in Lublin, Gliniana Str. 33/51, 20-031 Lublin, Poland

\* Correspondence: monika.wawrzkievicz@mail.umcs.pl; Tel.: +48-81-537-57-38

**Abstract:** This article presents the synthesis and sorption characteristics of novel microspheres based on 4-vinylbenzene chloride (VBCl) with divinylbenzene (DVB) or ethylene glycol dimethylacrylate (EGDMA). To confirm the chemical structure of the homo- and co-polymers attenuated total reflectance, Fourier transform infrared spectroscopy (ATR-FTIR) was used. The presence of characteristic functional groups (–OH, –CH, –CH<sub>2</sub>, C–O, C=O and C–O–C) in obtained microspheres was confirmed. Differential scanning calorimetry (DSC) analysis confirms the good thermal resistance of the polymers. The decomposition of microspheres is closely related to the chemical structure of the monomers used. DVB-derived materials decompose in one step, whereas the decomposition of EGDMA derivatives is multi-stage. Obtained polymeric microspheres were applied for auramine O (AO) basic dye removal from aqueous solutions. Equilibrium studies confirmed that the Freundlich model described the system better than Langmuir or Temkin equations and the adsorption capacities  $k_F$  ranged from 4.56 to 7.85 mg<sup>1–1/n</sup> L<sup>1/n</sup>/g. The sorption kinetic of AO from solutions of the 10 and 100 mg/L concentrations was very fast, and after 10 min, equilibrium was reached.



**Citation:** Wawrzkievicz, M.; Podkościelna, B. Innovative Polymer Microspheres with Chloride Groups Synthesis, Characterization and Application for Dye Removal. *Processes* **2022**, *10*, 1568. <https://doi.org/10.3390/pr10081568>

Academic Editor: Katherine M. E. Stewart

Received: 15 July 2022

Accepted: 9 August 2022

Published: 10 August 2022

**Publisher's Note:** MDPI stays neutral with regard to jurisdictional claims in published maps and institutional affiliations.



**Copyright:** © 2022 by the authors. Licensee MDPI, Basel, Switzerland. This article is an open access article distributed under the terms and conditions of the Creative Commons Attribution (CC BY) license (<https://creativecommons.org/licenses/by/4.0/>).

**Keywords:** 4-vinylbenzene chloride; polymeric microspheres; auramine O; dyes sorption; textile wastewaters

## 1. Introduction

Dyes, especially of the diphenyl methane class, are widely used in various industries for direct dyeing of wool, natural silk, polyacrylonitrile and hemp fibers and, formerly, cotton after mordanting, as well as for paper, wood and leather dyeing. There are currently more than 100,000 known types of dye available commercially [1]. Their annual production is estimated at more than  $7 \times 10^5$  tons [1–5]. Approximately 10–15% of the quantity of dyes used in the dyeing process is not bound by the fibers of the dyed materials and may enter the aquatic environment with the wastewater [2–4]. The widespread use of dyes is linked to the problem of their contamination of surface water in industrialized areas. In reservoirs and watercourses, they alter colour, reduce primary production, cause oxygen deficits and deteriorate living conditions [2,3]. Most dyes are characterized by high toxicity, mutagenicity and low biodegradability [4–6]. It is worth mentioning that commonly used synthetic dyes, such as ring-structured compounds, are degradable with the formation of dangerous and toxic intermediates [6].

One effective method for removing dyes from water and wastewater, both in the low and high concentration range, is their adsorption onto porous synthetic sorbents (e.g., activated carbons, ion exchange resins) [7,8]. However, high manufacturing costs and problems with regeneration of used carbon or ion exchangers necessitate the search for effective and economical sorbents, of both mineral and organic origin, with high efficiency in binding dyes from wastewater [9–11]. Knowledge of the sorption capacity of newly synthesized adsorbent materials in relation to dyes and their binding mechanism is of great importance in

technological processes of wastewater treatment, and is also necessary for the optimization of sorption processes for specific real-world conditions and in the design of new, effective and economical sorbents [12]. The continual tightening of permissible pollutant concentration limits has meant that work on assessing the properties of adsorbents is currently very intensive, as evidenced by the extensive literature [11–14]. The present study is also part of this research. Polymer resins used in wastewater treatment processes are commonly prepared from the styrene and varying amounts of a crosslinking agent, most commonly divinylbenzene [15], which controls the porosity of the particles. Popular resins available on the market are acrylic [16], epoxy or phenol-formaldehyde [17] type. A common choice is between styrene-divinylbenzene copolymer and acrylic-divinylbenzene copolymer [15–17]. Polymeric microspheric sorbents based on divinylbenzene-crosslinked styrene, despite their many advantages including stability over the whole pH range, also have some limitations due to their hydrophobic nature. Structural characteristics (i.e., porosity) aside, the styrene matrix is stronger than the acrylic one, but it is less flexible than the more rigid styrene-based copolymer. The elasticity of the acrylic matrix is a desirable characteristic when it concerns the kinetics of contaminant adsorption, but it can be somewhat problematic when resin columns are subjected to wastewater flowing under significant pressure. In addition, polystyrene resins are more resistant to high temperatures than acrylate-based resins. However, an important feature of polyacrylic resins is their resistance to organic fouling.

An attempt to synthesize a new resin based on hydroxypropylmethacrylate-co-ethyleneglycol dimethacrylate-co-glycidylmethacrylate) terpolymer (HPMA-co-EGDMA-co-GMA via suspension polymerization for the removal of disperse dyes was undertaken by Bayramoglu et al. [18]. Poly(chlorobenzalimino thiourea amide) (PCBA) resin was synthesized by using the phosphorylation polycondensation method not only for dyes (methyl orange and acid orange) but also heavy metal ions ( $\text{Ni}^{2+}$  and  $\text{Zn}^{2+}$ ) removal [19]. Chelating resin poly(MMA-co-MA) was synthesized by radical polymerization of maleic anhydride (MA) and methyl methacrylate (MMA) and applied for azo dyes (Acid Yellow 42, acid Red 151 and Methylene Blue 9) removal [20].

The aim of our research was to obtain novel polymeric microspheres with a more hydrophilic character by using the suspension polymerization method. Therefore, instead of styrene, two functional monomers, EGDMA and VBCI, were used in our studies. Due to the application of functional monomers with more hydrophilic character, specific polymeric adsorbents were obtained. The influence of the functional groups on the physicochemical properties as well as adsorption behaviour for the auramine O removal was evaluated. Auramine O is a basic dye extensively used for the colouration of silk, cotton, leather and paper and in the preparation of pigment lakes and can therefore leach into the wastewater from dyeing baths and pose a risk to the environment.

## 2. Materials and Methods

### 2.1. Chemicals and Eluents

Poly(vinyl alcohol) (APV,  $M_w = 72,000$ ), ethylene glycol dimethylacrylate (EGDMA) and divinylbenzene (DVB) were purchased from Merck (Darmstadt, Germany).  $\alpha, \alpha'$ -Azoiso-bis-butyrionitrile (AIBN) was obtained from Fluka (Buchs, Switzerland). Toluene, octane, acetone, tetrahydrofurane (THF), chloroform ( $\text{CHCl}_3$ ), methanol (MeOH),  $\text{CaCl}_2$  and chlorobenzene (Ph-Cl) were bought in Avantor Performance Materials Poland S.A. (Gliwice, Poland).

The cationic dye auramine O of diphenyl methane class was chosen as the adsorbate (Classic Dyestuff Inc., High Point, NC, USA). It was purchased as yellow powder. It is soluble in water and ethanol. The dye structure and properties are presented in Figure 1. The stock solution of the dye of the initial concentration  $C_0 = 1000 \text{ mg/L}$  was prepared in distilled water. The working solutions were prepared by diluting the stock solution.

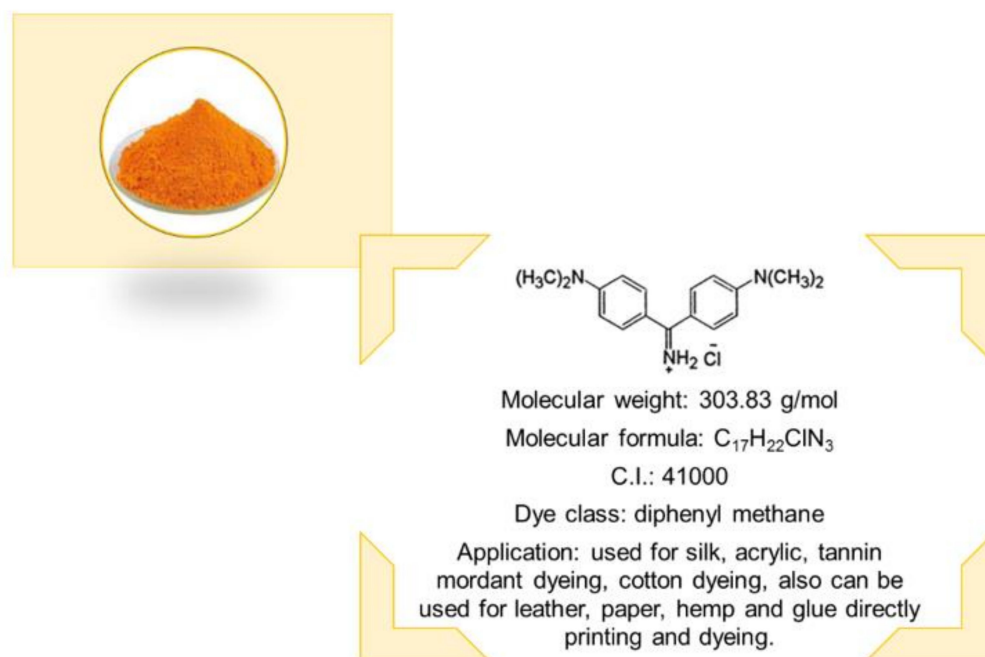


**Figure 1.** Properties of auramine O.

## 2.2. Preparation of Functional Microspheres

A total of 1.0 g suspension stabilizer (APV), 5 g CaCl<sub>2</sub> and purified water (150 mL) were placed in a 250 mL three-necked flask with a thermometer, a mechanical stirrer and an air condenser. The mixture was stirred to dissolve the suspension stabilizer for 1 h at 85 °C. Next, the monomers EGDMA or DVB and VBCl dissolved in porous solvents (20 mL toluene +5 mL octane) were added to water phase (see Table 1). The initiator (AIBN) was added to the organic phase in an amount of 1 wt.% of monomers. The mixture was stirred at 300 rpm for 8 h at 85 °C. The obtained polymeric microspheres were filtered off and washed with distilled hot water (1.5 L). The chemical structure of monomers used are presented in Figure 2.

**Table 1.** Experimental conditions of synthesis.

Copolymer	VBCl (g)	DVB (g)	EGDMA (g)	AIBN (g)
poly(DVB)	0	20	0	0.200
DVB-VBCl	11.69	10	0	0.217
poly(EGDMA)	0	0	20	0.200
EGDMA-VBCl	7.67	0	10	0.176

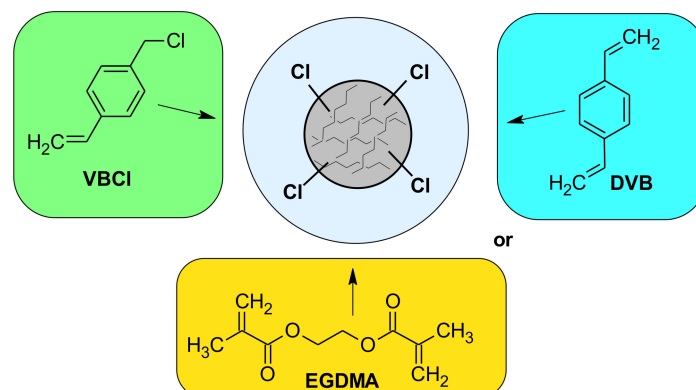


**Figure 2.** Chemical structure of monomers.

### 2.3. Measurements

The Fourier transform infrared (FT-IR) spectra were recorded with a Bruker Tensor 27 FTIR spectrometer (Bruker Co., Leipzig, Germany) using the attenuated total reflectance (ATR) technique. All spectra were obtained at room temperature after averaging 32 scans between 600 and 4000  $\text{cm}^{-1}$  with a resolution of 4  $\text{cm}^{-1}$  in the absorbance mode.

The calorimetric measurements were carried out in a DSC 204, Netzsch calorimeter (Netzsch GmbH, Weimar, Germany) operated in a dynamic mode. The dynamic scans were performed at a heating rate of 10  $^{\circ}\text{C min}^{-1}$ , from  $-10^{\circ}\text{C}$  to  $500^{\circ}\text{C}$  in a nitrogen atmosphere (30 mL/min). The mass of the sample was between 5 and 10 mg. An empty aluminum crucible was used as a reference.

Photos of the microspheres were studied using the optical microscope Morphologi G3 (Malvern, Great Britain, UK).

### 2.4. Batch Adsorption Test

Adsorption tests were carried out as follows: 0.02 g of the poly(DVB), DVB-VBCL, poly(EGDMA), or EGDMA-VBCL was weighed out in a 100 mL Erlenmayer flask, and 20 mL of auramine O solution of the specified concentration was poured in. The flasks were shaken on a mechanical shaker Elpin 358+ (Elpin, Lubawa, Poland) for 24 h (equilibrium test) or from 1 to 120 min (kinetic test) at room temperature ( $25^{\circ}\text{C}$ ). The AO solutions were filtered after sorption experiments and dye concentration was measured using the UV-Vis spectrophotometry Cary 60 (Agilent, Santa Clara, CA, USA) at the maximum wavelengths 430 nm. All adsorption experiments were performed in triplicates and the mean values were used for data evaluation. The standard deviation did not exceed 3%. The amounts of AO adsorbed by the poly(DVB), DVB-VBCL, poly(EGDMA) and EGDMA-VBCL microspheres at equilibrium ( $q_e$ ) and at time  $t$  ( $q_t$ ) were calculated from the following formulas:

$$q_e = \frac{(C_0 - C_e)}{m} \cdot V \quad (1)$$

$$q_t = \frac{(C_0 - C_t)}{m} \cdot V \quad (2)$$

where:  $C_0$ ,  $C_e$  and  $C_t$  (mg/L)—AO concentrations in the solution before adsorption, at equilibrium and after sorption time  $t$ , respectively,  $V$  (L)—volume of the solution, and  $m$  (g)—mass of the adsorbent.

## 3. Results

### 3.1. Visualization of Microspheres

In Figure 3, the photos of the obtained microspheres are presented. All materials are characterized by spherical shape but with different sizes. The addition of VBCL to DVB significantly reduces the diameter of the microspheres (ca. 50%). This effect is not visible for EGDMA derivatives. The most homogeneous material with regards to the microsphere size was obtained for poly(DVB) and approximately 90% of the material is in the range of 360–400  $\mu\text{m}$ .

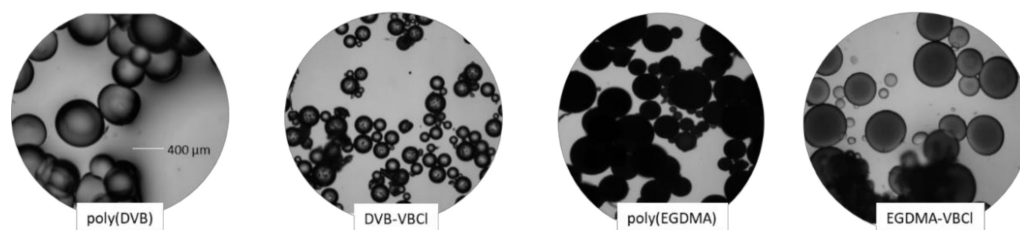


**Figure 3.** Photos of the synthesized microspheres.

After the addition of VBCI, the diameter of the microspheres changes, and they are in the range of 180–220  $\mu\text{m}$ . In the case of EGDMA derivatives, the diameter dispersion is slightly larger, and approximately 80% of the material is in the range of 350–400  $\mu\text{m}$ .

### 3.2. ATR-FTIR Spectroscopy

The ATR-FTIR spectra for the obtained microspheres are presented in Figure 4. In all spectras, except poly(DVB), hydroxyl groups ranging from 3500–3300  $\text{cm}^{-1}$  are visible. The broad absorption band indicates the presence of –OH groups from solvents and water. The stretching vibrations for the C–H groups appeared at 2860  $\text{cm}^{-1}$ . The signal at 1447  $\text{cm}^{-1}$  for poly(DVB) and the signal at 1445  $\text{cm}^{-1}$  for DVB-VBCI are from C–H deformation in the –CH<sub>2</sub> groups. In the poly(DVB) at the range of 900–800  $\text{cm}^{-1}$  and at 793  $\text{cm}^{-1}$ , isolated aromatic C–H groups vibrations are noticeable. The signal in range 707  $\text{cm}^{-1}$ –704  $\text{cm}^{-1}$  for the both materials can be attributed to C=C vibrations of aromatic bands.

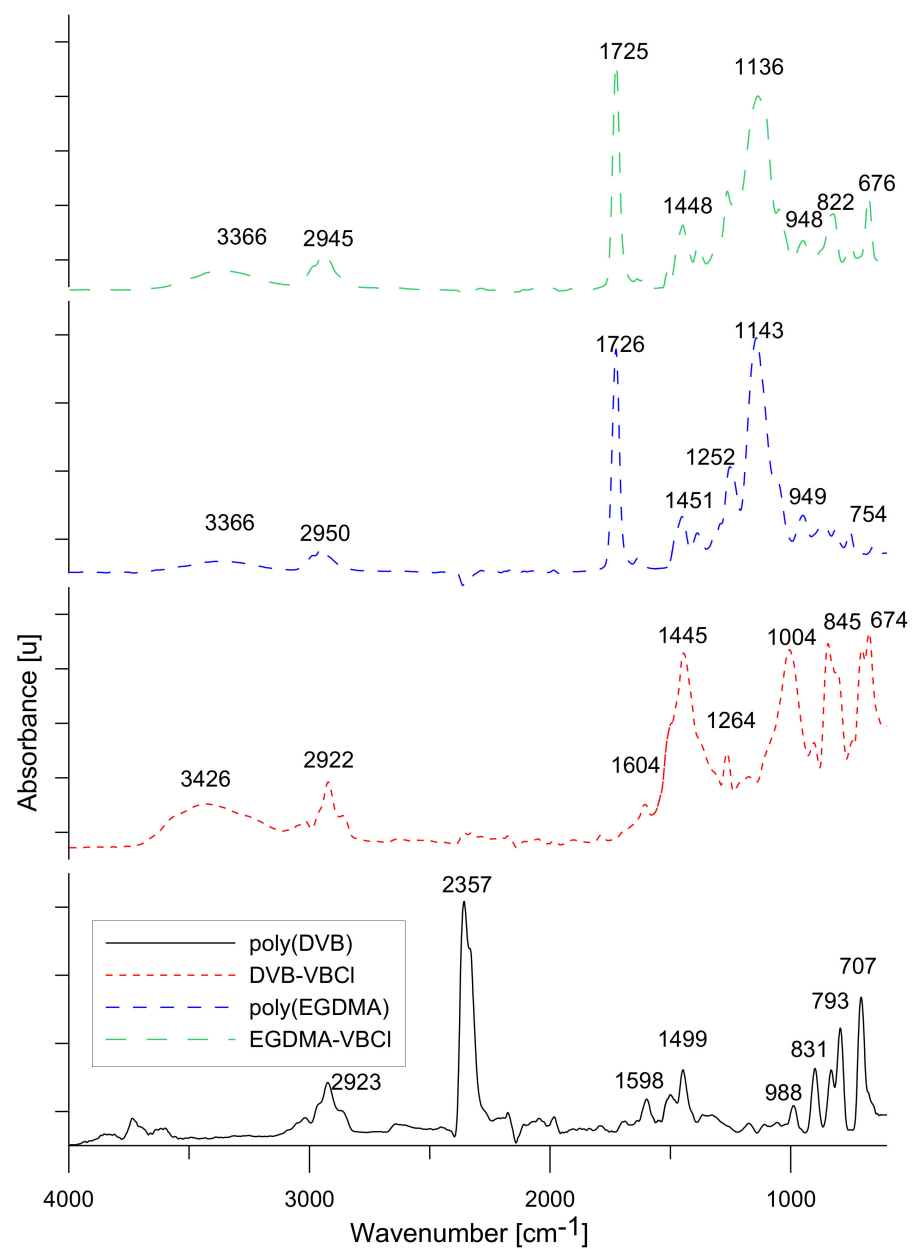
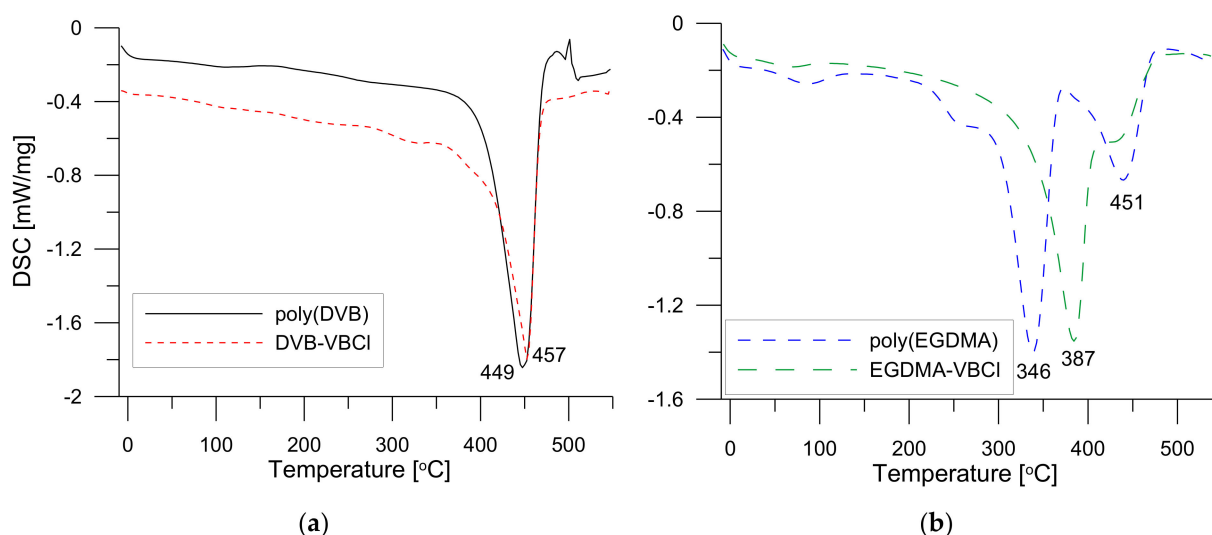


Figure 4. ATR-FTIR spectra of the studied materials.

For the spectra, for EGDMA derivatives, the characteristic signal at  $2950\text{ cm}^{-1}$  for poly(EGDMA) and  $2945\text{ cm}^{-1}$  for EGDMA-VBCL is derived from the stretching vibrations from C–H aliphatic groups. The signal at  $1726\text{ cm}^{-1}$  and  $1725\text{ cm}^{-1}$  for both derivatives indicates the vibrations of C=O group from EGDMA. The signals at  $1451\text{ cm}^{-1}$  and at  $1448\text{ cm}^{-1}$  seem to be from the vibrations of C–H groups. The  $1388$  and  $1384\text{ cm}^{-1}$  signals are from the C–H deformation vibrations from  $-\text{CH}_3$  and  $-\text{CH}_2$  groups. Furthermore, the signals around  $1252$  and  $1263\text{ cm}^{-1}$  indicate C–O stretching vibrations. The signal at  $822\text{ cm}^{-1}$  corresponds to the C–H aromatic vibrations from EGDMA-VBCL.

### 3.3. DSC Analysis

In Figure 5a,b, the DSC curves in the range of  $-10$  to  $500$  are visible. Analysing the course of the curves for DVB derivatives, one can see that no significant changes up to ca.  $380\text{ }^\circ\text{C}$  are visible. In the graphs, one endothermic effect with the maximum at  $449\text{--}457\text{ }^\circ\text{C}$  is observed. This endothermic effect is connected with the degradation of the samples. In contrast, some differences related to the course of curves for the EGDMA based materials can be seen. Two small effects at ca.  $80\text{--}100\text{ }^\circ\text{C}$  and  $280\text{ }^\circ\text{C}$  for poly(EGDMA) related with the loss of water and degradation of small aliphatic polymer fragments are noted. On the curves, two larger effects ( $346\text{--}387$  and ca.  $450\text{ }^\circ\text{C}$ ) related to the total degradation of the crosslinked chains and the aromatic fragments of VBCL are evident. Generally, the addition of VBCL to the EGDMA monomer improves the thermal resistance of the sample.



**Figure 5.** DSC curves of (a) poly(DVB) and DVB-VBCL as well as (b) poly(EGDMA) and EGDMA-VBCL.

### 3.4. Batch Adsorption Test

#### 3.4.1. Sorption Capacities

The process of dye adsorption on the poly(DVB), DVB-VBCL, poly(EGDMA) and EGDMA-VBCL microspheres was carried out using a static method. It involves determining the difference in concentrations of the dye in the solutions before and after adsorption. For this purpose, a known amount of adsorbent was introduced into a defined volume of dye solution and mixed at a constant temperature until equilibrium of the process was reached. This allows the adsorption capacity to be determined. The experimental equilibrium data were modelled using linear forms of the Langmuir (Equation (3)), Freundlich (Equation (4)) and Temkin (Equation (5)) isotherm models [21,22]:

$$\frac{C_e}{q_e} = \frac{1}{Q_0 k_L} + \frac{C_e}{Q_0} \quad (3)$$

$$\log q_e = \log k_F + \frac{1}{n} \log C_e \quad (4)$$

$$q_e = \left( \frac{RT}{b_T} \right) \ln A + \left( \frac{RT}{b_T} \right) \ln C_e \quad (5)$$

where  $q_e$ —the adsorption capacity (mg/g),  $C_e$ —the equilibrium concentration of solution (mg/L),  $Q_0$ —the monolayer adsorption capacity (mg/g),  $k_L$ —the Langmuir constant (related to the free energy of adsorption) (L/mg),  $k_F$  ( $\text{mg}^{1-1/n} \text{L}^{1/n}/\text{g}$ ),  $1/n$ —the Freundlich constants connected with adsorption capacity of adsorbent and the surface heterogeneity, respectively,  $R$ —the gas constant (8.314 J/mol K),  $T$ —the temperature (K),  $A$  (L/g) and  $b_T$  (J/mol)—the Temkin constants.

The isotherm parameters were calculated from the slopes and intercepts of the  $C_e/q_e$  vs.  $C_e$ ,  $\log q_e$  vs.  $\log C_e$  and  $q_e$  vs.  $\ln C_e$  plots ( $Q_0 = 1/\text{slope}$ ,  $b = \text{slope}/\text{intercept}$ ,  $1/n = \text{slope}$ ,  $k_F = 10^{\text{intercept}}$ ,  $b_T = RT/\text{slope}$ ,  $A = \exp(\text{intercept}/\text{slope})$ ) and are listed in Table 2.

**Table 2.** The parameters of Langmuir, Freundlich and Temkin isotherm models calculated using linear regression for the investigated adsorption systems.

Isotherm Model	Parameters	poly(DVB)	DVB-VBCL	poly(EGDMA)	EGDMA-VBCL
Langmuir	$Q_0$ (mg/g)	141.7	239.3	81.0	93.9
	$k_L$ (L/mg)	0.033	0.019	0.106	0.067
	$R^2$	0.549	0.149	0.399	0.669
Freundlich	$k_F$ ( $\text{mg}^{1-1/n} \text{L}^{1/n}/\text{g}$ )	4.56	4.97	7.85	5.80
	$1/n$	0.910	0.919	0.732	0.846
	$R^2$	0.995	0.989	0.980	0.997
Temkin	$b_T$ (J g/mol mg)	294.3	296.5	359.1	308.7
	$A$ (L/mg)	2.62	2.66	7.02	3.62
	$R^2$	0.767	0.725	0.664	0.756

The adsorption isotherms of AO on the poly(DVB), DVB-VBCL, poly(EGDMA) and EGDMA-VBCL microspheres are shown in Figure 6. Fitting lines corresponding to the three adsorption isotherms indicate that the Freundlich model seems to be the best one. The Freundlich isotherm is an empirical model which is widely applied to describe heterogeneous systems, especially adsorption of organic compounds. The determination coefficients for the Freundlich model were found to be in the range 0.980–0.997. The  $k_F$  values were ranged from 4.56 to 7.85  $\text{mg}^{1-1/n} \text{L}^{1/n}/\text{g}$ . The  $1/n$  parameters describing the intensity of adsorption were below in the investigated system and prove favorable uptake of AO by the poly(DVB), DVB-VBCL, poly(EGDMA) and EGDMA-VBCL microspheres (unfavorable adsorption  $1/n > 1$ ).

The Langmuir isotherm assumes that an adsorbate (i.e., AO dye) can form a monolayer of molecules on the surface of an adsorbent (i.e., polymeric microspheres), interacting with adsorption sites and not interacting with each other. The Temkin isotherm equation, on the other hand, assumes that the heat of adsorption of all dye molecules in the layer would decrease linearly due to the adsorbent-adsorbate interaction; moreover, adsorption is characterized by a uniform distribution of binding energy. Considering AO adsorption on poly(DVB), DVB-VBCL, poly(EGDMA) and EGDMA-VBCL, it can be seen that the Langmuir and Temkin models provided an unsatisfactory description of experimental data. The values of the determination coefficients  $R^2$  for the Langmuir model ranged from 0.149 to 0.669 and from 0.664 to 0.767 for the Temkin model. These values were smaller than those determined for the Freundlich model.

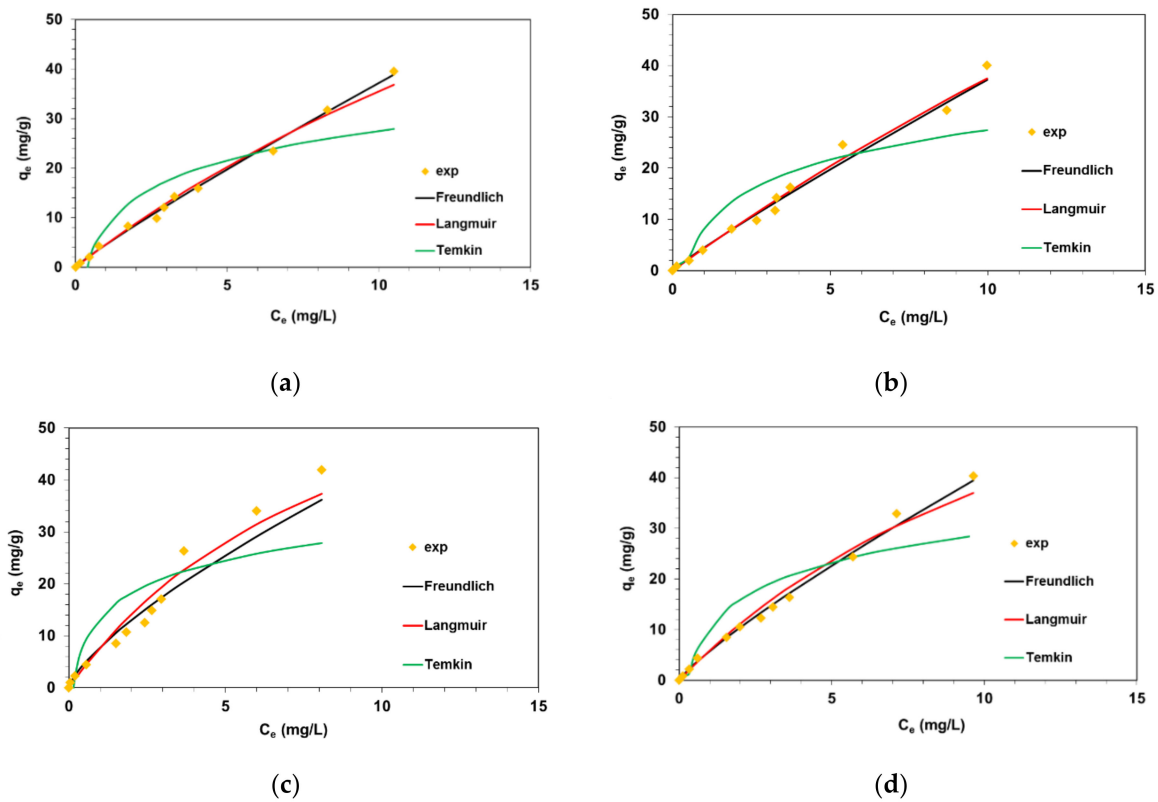


**Figure 6.** Fitting of isotherm models to the AO dye adsorption equilibrium data on (a) poly(DVB), (b) DVB-VBCL, (c) poly(EGDMA) and (d) EGDMA-VBCL.

Considering the parameters of the adsorption isotherms and their fit to experimental data, it can be concluded that adsorption mechanisms involve mainly weak  $\pi$ - $\pi$  interactions between the aromatic rings of the poly(DVB), DVB-VBCL, poly(EGDMA), EGDMA-VBCL and the benzene rings present in the dye structure as well as electrostatic interactions involving positively charged AO cations and chloride or oxygen anions as presented in Figure 7.

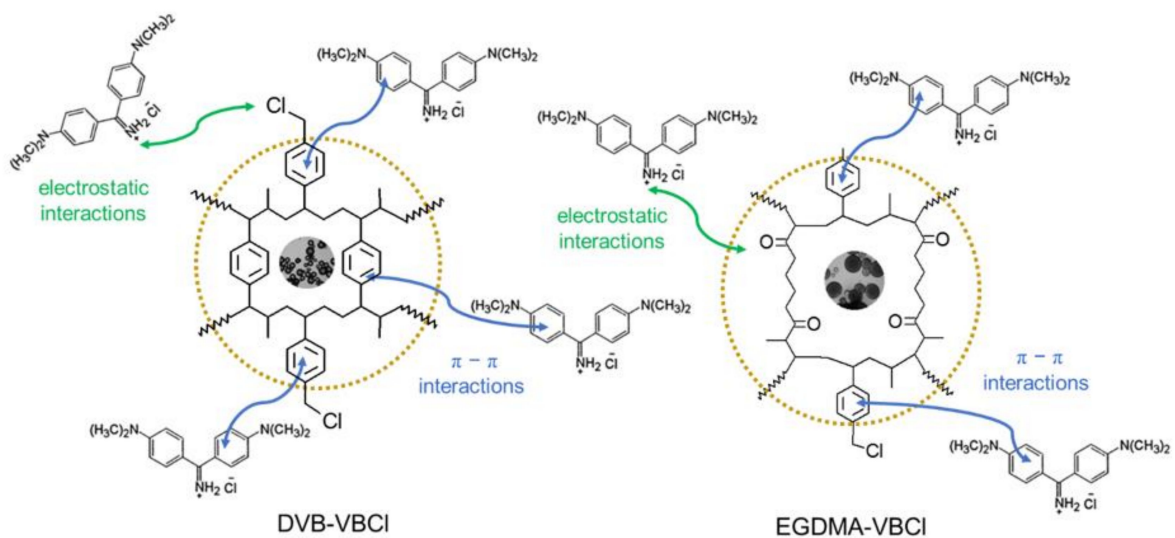


**Figure 7.** Proposed mechanism of interactions between AO dye and the DVB-VBCL and EGDMA-VBCL microspheres.



The sorption capacities obtained at equilibrium, along with the most appropriate isotherm model describing the sorption process of AO on the polymeric microspheres, were compared with the available literature data and are summarized in Table 3.

**Table 3.** Removal of auramine O by different adsorbents based on the literature review.

Adsorbent	Equilibrium Data	Ref.
Clay mineral from Turkey	Langmuir model: $q_e = 833.3\text{--}714.28 \text{ mg/g}$ at 25–45 °C	[23]
Bagasse fly ash	Langmuir model: $q_e = 31.18 \text{ mg/g}$ at 30 °C	[24]
Mesoporous carbons	Langmuir model: $q_e = 175\text{--}360 \text{ mg/g}$ at 30–60 °C	[25]
C/SiO <sub>2</sub> composite	Freundlich model: $k_F = 27.37\text{--}55.41 \text{ mg}^{1-1/n} \text{ L}^{1/n}/\text{g}$ T = 20–60 °C,	[26]
EGDMA + DVB	Freundlich model: $k_F = 11.1\text{--}45.7 \text{ mg}^{1-1/n} \text{ L}^{1/n}/\text{g}$	[27]
+ TEVS + ZrO <sub>2</sub> – SiO <sub>2</sub> + Lignin	at 20–60 °C	
Modified globe <i>Artichoke</i> leaves	Langmuir model: $q_e = 344.8 \text{ mg/g}$ at 25 °C	[28]
poly(DVB), DVB-VBCL, poly(EGDMA), EGDMA-VBCL	Freundlich model: $k_F = 4.56\text{--}7.85 \text{ mg}^{1-1/n} \text{ L}^{1/n}/\text{g}$ at 25 °C	This study

### 3.4.2. Kinetic Studies

When evaluating the amount of AO dye retained by the synthesized adsorbents, an extremely important step in the study was the selection of process conditions, i.e., phase contact time. In the kinetic adsorption tests carried out, the range of the tested parameters varied from 1 min to 240 min for two different concentrations of AO (10 and 100 mg/L) in solution. Figure 8 shows a graphical interpretation of the  $q_t$  vs.  $t$ , confirming the high affinity of AO for poly(DVB), DVB-VBCL, poly(EGDMA) and EGDMA-VBCL. The result is the almost immediate establishment of the adsorption equilibrium in the studied systems. After 10 min of phase contact time, the amount of AO taken up by the polymer microspheres reached maximum values. Slightly bigger  $q_t$  values were obtained for DVB-VBCL and EGDMA-VBCL adsorbents. The amount of adsorbed AO by EGDMA-based sorbents is insignificantly greater than that of DVB-based sorbents, which may be due to the more hydrophilicity of the former.

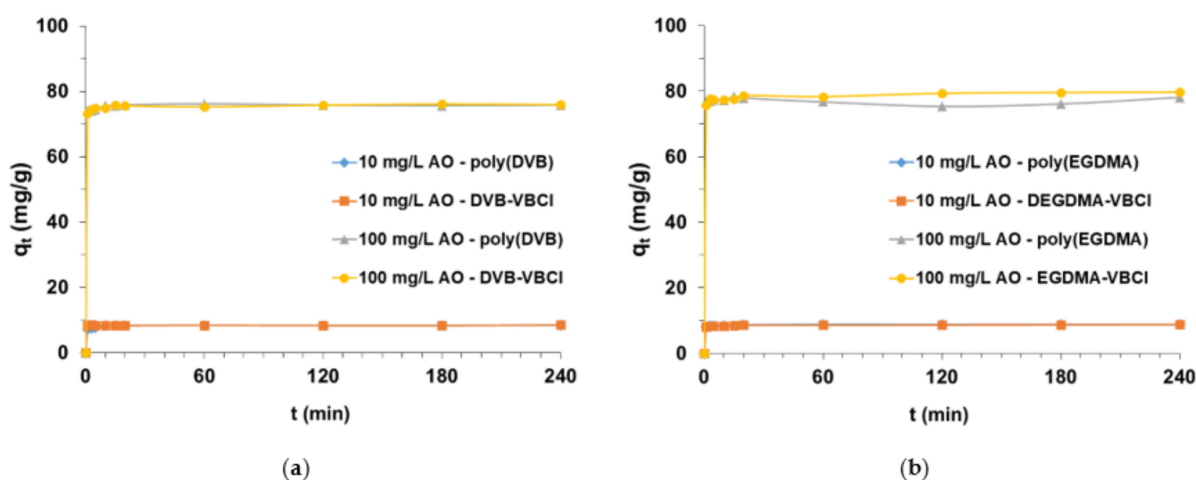


**Figure 8.** Time impact on AO uptake from the solutions of initial concentrations 10 mg/L and 100 mg/L by (a) poly(DVB) and DVB-VBCL as well as (b) poly(EGDMA) and EGDMA-VBCL.

Comparing the results obtained with the data available in the literature, it should be noted that the optimal phase contact time of the adsorption process is strongly determined

by the type of adsorbent used. For example, the time necessary to reach equilibrium in the solutions containing AO in the amount of 50 mg/L using the EGDMA + DVB + TEVS + ZrO<sub>2</sub>-SiO<sub>2</sub> + lignin based adsorbents was found to be 180 min. After 1 min of phase contact time, about 81.1–85.7% of AO was removed by EGDMA + DVB + TEVS + ZrO<sub>2</sub> – SiO<sub>2</sub> + lignin based adsorbents [27]. According to Şenol et al. [29] investigating AO retention (500 mg/L) using epichlorohydrin and tripolyphosphate-crosslinked chitosan-kaolin composite by after the 6 h, an equilibrium plateau was reached and maintained until the 24 h. During AO (100 mg/L) sorption experiments on *Ipomoea aquatica* roots as ecofriendly adsorbent, 120 min was sufficient for the system to reach equilibrium [30]. Liu et al. [31] reported that 3 h was enough to obtain the equilibrium during AO (50–200 mg/L) sorption on the sesame leaf as a biosorbent.

#### 4. Conclusions

The paper presents synthesis of the new polymer microspheres with chloride groups such as DVB-VBCL and EGDMA-VBCL and their application for toxic auramine O dye removal. Properties of the adsorbents were compared with poly(DVB) and poly(EGDMA). ATR-FTIR spectra confirmed the appearance of characteristic groups present in the structure of the monomers used such as: C–H at 2860 cm<sup>-1</sup>, Ph at 900–800, 790, 700 cm<sup>-1</sup>, C=O at 1725 cm<sup>-1</sup> and C=O at 1250–1260 cm<sup>-1</sup>. DSC analysis proved that the addition of VBCL to the microspheres structure improves the thermal properties. The DSC curves for DVB derivatives were characterised by a single main endothermic effect around 450 °C, whereas EGDMA degrades in three steps. The addition of VBCL results in an increase in thermal resistance of these materials ca. 40 °C. AO uptake by poly(DVB), DVB-VBCL, poly(EGDMA) and EGDMA-VBCL was very fast, and the equilibrium retention of the dye was observed after 10 min of phase contact time. The determination coefficients for the Freundlich model being in the range of 0.980–0.997 confirmed applicability of the model in the description of the experimental data compared with the Langmuir or Temkin equations.

**Author Contributions:** Conceptualization, M.W. and B.P.; methodology, M.W. and B.P.; software, M.W. and B.P.; formal analysis, M.W. and B.P.; investigation, M.W. and B.P.; resources, M.W. and B.P.; data curation, M.W. and B.P.; writing—original draft preparation, M.W. and B.P.; writing—review and editing, M.W. and B.P.; visualization, M.W. and B.P.; supervision, M.W. and B.P.; All authors have read and agreed to the published version of the manuscript.

**Funding:** This research received no external funding.

**Institutional Review Board Statement:** Not applicable.

**Informed Consent Statement:** Not applicable.

**Data Availability Statement:** MDPI Research Data Policies.

**Acknowledgments:** The authors would like to thank Agnieszka Lipke, from the Institute of Chemical Sciences at Maria Curie-Skłodowska University in Lublin for her help in carrying out laboratory work on adsorption.

**Conflicts of Interest:** The authors declare no conflict of interest. The funders had no role in the design of the study; in the collection, analyses or interpretation of data; in the writing of the manuscript, or in the decision to publish the results.

#### References

1. Martins, L.R.; Rodrigues, J.A.V.; Adarme, O.F.H.; Melo, T.M.S.; Gurgel, L.V.A.; Gil, L.F. Optimization of cellulose and sugarcane bagasse oxidation: Application for adsorptive removal of crystal violet and auramine-O from aqueous solution. *J. Colloid Interface Sci.* **2017**, *494*, 223–241. [[CrossRef](#)] [[PubMed](#)]
2. Carneiro, M.T.; Barros, A.Z.B.; Morais, A.I.S.; Carvalho Melo, A.L.F.; Bezerra, R.D.S.; Osajima, J.A.; Silva-Filho, E.C. Application of water hyacinth biomass (*Eichhornia crassipes*) as an adsorbent for methylene blue dye from aqueous medium: Kinetic and isothermal study. *Polymers* **2022**, *14*, 2732. [[CrossRef](#)] [[PubMed](#)]
3. Wang, X.; Zhang, P.; Xu, F.; Sun, B.; Hong, G.; Bao, L. Adsorption of methylene blue on azo dye wastewater by molybdenum disulfide nanomaterials. *Sustainability* **2022**, *14*, 7585. [[CrossRef](#)]

4. Lara, L.; Cabral, I.; Cunha, J. Ecological approaches to textile dyeing: A Review. *Sustainability* **2022**, *14*, 8353. [[CrossRef](#)]
5. Wawrzekiewicz, M.; Wołowicz, A.; Hubicki, Z. Strongly basic anion exchange resin based on a cross-linked polyacrylate for simultaneous C.I. Acid Green 16, Zn(II), Cu(II), Ni(II) and phenol removal. *Molecules* **2022**, *27*, 2096. [[CrossRef](#)]
6. Tkaczyk, A.; Mitrowska, K.; Posyniak, A. Synthetic organic dyes as contaminants of the aquatic environment and their implications for ecosystems: A review. *Sci. Total Environ.* **2020**, *117*, 137222. [[CrossRef](#)]
7. Podkościelna, B.; Kołodyńska, D. A new type of cation-exchange polymeric microspheres with pendant methylenethiol groups. *Polym. Adv. Technol.* **2013**, *24*, 866–872. [[CrossRef](#)]
8. Goliszek, M.; Podkościelna, B.; Fila, K.; Riazanova, A.V.; Aminzadeh, S.; Sevastyanova, O.; Gun'ko, V.M. Synthesis and structure characterization of polymeric nanoporous microspheres with lignin. *Cellulose* **2018**, *25*, 5843–5862. [[CrossRef](#)]
9. Wawrzekiewicz, M.; Podkościelna, B.; Podkościelny, P. Application of functionalized DVB-co-GMA polymeric microspheres in the enhanced sorption process of hazardous dyes from dyeing baths. *Molecules* **2020**, *25*, 5247. [[CrossRef](#)]
10. Yagub, M.T.; Sen, T.K.; Afroze, S.; Ang, H.M. Dye and its removal from aqueous solution by adsorption: A review. *Adv. Colloid Interface Sci.* **2014**, *209*, 172–184. [[CrossRef](#)]
11. Dutta, S.; Gupta, B.; Srivastava, S.K.; Gupta, A.K. Recent advances on the removal of dyes from wastewater using various adsorbents: A critical review. *Mater. Adv.* **2021**, *2*, 4497. [[CrossRef](#)]
12. Elgarahy, A.M.; Elwakeel, K.Z.; Mohammad, S.H.; Elshoubaky, G.A. A critical review of biosorption of dyes, heavy metals and metalloids from wastewater as an efficient and green process. *Clean. Eng. Technol.* **2021**, *4*, 100209. [[CrossRef](#)]
13. Badawi, A.K.; Elkodous, M.A.; Ali, G.M.A. Recent advances in dye and metal ion removal using efficient adsorbents and novel nano-based materials: An overview. *RSC Adv.* **2021**, *11*, 36528–36553. [[CrossRef](#)]
14. Katheresan, V.; Kannedo, J.; Lau, S.Y. Efficiency of various recent wastewater dye removal methods: A review. *J. Environ. Chem. Eng.* **2018**, *6*, 4676–4697. [[CrossRef](#)]
15. Wawrzekiewicz, M. Application of weak base anion exchanger in sorption of tartrazine from aqueous medium. *Solvent Extr. Ion Exch.* **2010**, *28*, 845–863. [[CrossRef](#)]
16. Wawrzekiewicz, M.; Hubicki, Z. Equilibrium and kinetic studies on the adsorption of acidic dye by the gel anion exchanger. *J. Hazard. Mater.* **2009**, *172*, 868–874. [[CrossRef](#)]
17. Wawrzekiewicz, M.; Hubicki, Z. Remazol Black B removal from aqueous solutions and wastewater using weakly basic anion exchange resins. *Cent. Eur. J. Chem.* **2011**, *9*, 867–876. [[CrossRef](#)]
18. Bayramoglu, G.; Kunduzcu, G.; Arica, M.Y. Preparation and characterization of strong cation exchange terpolymer resin as effective adsorbent for removal of disperse dyes. *Polym. Eng. Sci.* **2019**, *60*, 192–201. [[CrossRef](#)]
19. Vidhyadevi, T.; Arukkani, M.; Selvaraj, K.; Premkumar, M.P.; Ravikumar, L.; Sivanesan, S. A study on the removal of heavy metals and anionic dyes from aqueous solution by amorphous polyamide resin containing chlorobenzalimine and thioamide as chelating groups. *Korean J. Chem. Eng.* **2015**, *32*, 650–660. [[CrossRef](#)]
20. Masoumi, A.; Ghaemy, M. Adsorption of heavy metal ions and azo dyes by crosslinked nano-chelating resins based on poly(methylmethacrylate-co-maleic anhydride). *eXPRESS Polym. Lett.* **2014**, *8*, 187–196. [[CrossRef](#)]
21. Foo, K.Y.; Hameed, B.H. Insights into the modeling of adsorption isotherm systems. *Chem. Eng. J.* **2010**, *156*, 2–10. [[CrossRef](#)]
22. Mozaffari Majd, M.; Kordzadeh-Kermani, V.; Ghalandari, V.; Askari, A.; Sillanpää, M. Adsorption isotherm models: A comprehensive and systematic review (2010–2020). *Sci. Total Environ.* **2022**, *812*, 151334. [[CrossRef](#)] [[PubMed](#)]
23. Öztürk, A.; Malkoc, E. Adsorptive potential of cationic Basic Yellow 2 (BY2) dye onto natural untreated clay (NUC) from aqueous phase: Mass transfer analysis, kinetic and equilibrium profile. *Appl. Surf. Sci.* **2014**, *299*, 105–115. [[CrossRef](#)]
24. Mall, I.D.; Srivastava, V.C.; Agarwal, N.K. Adsorptive removal of auramine-O: Kinetic and equilibrium study. *J. Hazard. Mater.* **2007**, *143*, 386–395. [[CrossRef](#)] [[PubMed](#)]
25. Gościńska, J.; Marciniak, M.; Pietrzak, R. The effect of surface modification of mesoporous carbons on auramine-O dye removal from water. *Adsorption* **2015**, *22*, 531–540. [[CrossRef](#)]
26. Wiśniewska, M.; Wawrzekiewicz, M.; Onyszko, M.; Medykowska, M.; Nosal-Wiercińska, A.; Bogatyrov, V. Carbon-silica composite as adsorbent for removal of hazardous C.I. Basic Yellow 2 and C.I. Basic Blue 3 dyes. *Materials* **2021**, *14*, 3245. [[CrossRef](#)] [[PubMed](#)]
27. Wawrzekiewicz, M.; Podkościelna, B.; Jesionowski, T.; Kłapiszewski, Ł. Functionalized microspheres with co-participated lignin hybrids as a novel sorbents for toxic C.I. Basic Yellow 2 and C.I. Basic Blue 3 dyes removal from textile sewage. *Ind. Crops Prod.* **2022**, *180*, 114785. [[CrossRef](#)]
28. Laribi, K.; Sahmoune, M.N. Equilibrium studied of auramine O adsorption on modified globe *Artichoke* leaves. *Res. J. Chem. Environ. Sci.* **2016**, *4*, 44–52.
29. Şenol, Z.M.; Çetinkaya, S.; Yenidünya, A.F.; Başoğlu-Ünal, F.; Ece, A. Epichlorohydrin and tripolyphosphate-crosslinked chitosan-kaolin composite for auramine O dye removal from aqueous solutions: Experimental study and DFT calculations. *Int. J. Biol. Macromol.* **2022**, *199*, 318–330. [[CrossRef](#)]
30. YieChen, L.; Priyanthab, N.; Lim, L.B.L. *Ipomoea aquatica* roots as environmentally friendly and green adsorbent for efficient removal of Auramine O dye. *Surf. Interf.* **2020**, *20*, 100543.
31. Liu, L.-E.; Yu, F.; Liu, J.; Han, X.; Zhang, H.; Zhang, B. Removal of auramine O from aqueous solution using sesame leaf: Adsorption isotherm and kinetic studies. *Asian J. Chem.* **2013**, *25*, 1991–1998. [[CrossRef](#)]